University of Notre Dame

2018-2019

Notre Dame Rocket Team
Flight Readiness Review Addendum

NASA Student Launch 2019
UAV and Air Braking Payloads

Submitted March 25, 2019

365 Fitzpatrick Hall of Engineering
Notre Dame, IN 46556

Contents

List of Tables

List of Figures

Table 1: List of acronyms

Acronym	Meaning
ABS	Air Braking System
ACCST	Advanced Continuous Channel Shifting Technology
AGL	Above Ground Level
CFD	Computational Fluid Dynamics
CPU	Central Processing Unit
CRAM	Compact Removable Avionics Module
DSM	Digital Spectrum Modulation
ESC	Electronic Speed Controller
FEA	Future Excursion Area
FMEA	Failure Modes and Effects Analysis
FPS	Frames Per Second
FPV	First-Person View
IMU	Inertial Measurement Unit
LED	Light Emitting Diode
LiPo	Lithium Polymer
NDRT	Notre Dame Rocket Team
OpenCV	Open Source Computer Vision Library
OPTO	Optoisolator
PCB	Printed Circuit Board
PDB	Power Distribution Board
PID	Proportional-Integral-Derivative
PLA	Polylactic Acid
PWM	Pulse-Width Modulation
RC	Radio Controlled
RF	Radio Frequency
UAV	Unmanned Aerial Vehicle

1 Summary of FRR Addendum

1.1 Team Summary

School Name: University of Notre Dame

Team Name: Notre Dame Rocketry Team

Location: University of Notre Dame
365 Fitzpatrick Hall of Engineering
Notre Dame, IN 46556

Faculty Advisor: Dr. Aleksander Jemcov
Research Assistant Professor
Department of Aerospace and Mechanical Engineering
e: ajemcov@nd.edu
p: (574)631-7576

Graduate Student Advisor: Emma Farnan
PhD Candidate
Department of Aerospace and Mechanical Engineering
e: efarnan@nd.edu
p: (631)572-6091

Team Lead: Patrick Danielson
e: pdaniels@nd.edu
p: (937)760-4366

Safety Officer: James Cole
e: jcole8@nd.edu
p: (347)835-3922

Mentor: Dave Brunsting (NAR/TAR Level 2)
e: dacsmema@gmail.com
p: (269)838-4275.

NAR/TRA Section: TRA #12340, Michiana Rocketry

In addition, NDRT's mission includes building a program centered around NASA's experiential learning project that will offer 60+ undergraduates opportunities to grow as engineers by developing technical and professional skills not available in a traditional undergraduate curriculum. Finally, the team aims to inspire young minds in the South Bend community through hands on activities promoting STEM education and rocketry.

1.2 Purpose of Flight

The Notre Dame Rocketry Team conducted a single test flight on Saturday, March 23. The test flight described in this report was to serve as the Vehicle Demonstration Re-Flight as well as the Payload Demonstration Flight as deemed necessary per the FRR action items given to the team. The flight was intended to demonstrate that the fully active UAV and Air Braking System payloads met all NASA and team derived requirements for the competition. The following report describes the extent to which the team was able to meet these requirements in the context of the success and failures experienced during the test launch.

1.3 Flight Summary Information

The test flight was performed on Saturday, March 23, 2019 in Three Oaks, MI under the supervision of Michiana Rockery and the NDRT mentor. The launch day conditions were a temperature of 37° F, barometric pressure of 14.45 psi, and wind conditions of 5 mph blowing from the Northwest.

The vehicle was powered by a Cesaroni L-1395 motor. The final active version of the UAV payload was flown and the Air Braking System payload was in its active configuration. In addition, 32 ounces of ballast were flown in order to assist in meeting the altitude goal of 4,700 feet. The declared and predicted altitudes for this configuration is compared to the flight measured altitudes in Table 2. It is worth noting that the predicted altitude is for a non-braked flight. The vehicle is designed to overshoot the declared altitude and allow the air braking tabs to reduce the apogee to the target.

Table 2: Altitude Comparison

Altitude	Value [ft]
Declared	4,700.0
Predicted	5,211.0
Altimeter 1	5,200.6
Altimeter 2	5,182.9
Altimeter 3	5,188.2

There were several off-nominal events that occurred during the flight.

- The Air Braking System correctly detected burnout and extended the drag tabs into the airflow as designed. However, the tabs were retracted early as a result of the pressure sensor detecting a decrease in altitude and the system thinking apogee had been reached. While this is the appropriate response to apogee detection, and the action of extending the tabs did not destabilize the vehicle, the early detection of apogee is off-nominal and will be discussed later in this report.
- After a successful separation event and drogue deployment, the main parachute began to unwrap from the nomex bundle and began to get wrapped up by the shock cords. This prevented the main parachute from fully opening when the chute releases deployed at 500 feet above ground level (AGL). The entanglement of the chute is off-nominal and will be discussed later in this report. It is worth noting that the parachute flown was not the intended parachute per the design at FRR and the decision to fly under this chute will also be addressed later.
- As a result of the main parachute failing to fully deploy, the vehicle experienced off-nominal forces upon landing. This resulted in structural failure to internal components of the UAV deployment mechanism that prevented a full execution of the deployment sequence. A more detailed discussion of the damage is given later in this report, however, the retention of the UAV for this flight was successful and all damaged components are able to be repaired.

1.4 Changes made since FRR

1.4.1 Changes to Vehicle

The following changes were made to the launch vehicle and recovery system designs between the time of FRR and this test flight:

- The main parachute used in the March 22 launch was the 144 inch Iris Fruity Chute main parachute. The main parachute was changed from the 20 foot Rocketman parachute due to the vendor being unable to adhere to terms of the order and deliver the parachute by the agreed up time prior to the launch. The Fruity Chute parachute has 36 shroud lines instead of the Rocketman parachute's 4. There was therefore an increased chance of shroud lines becoming tangled. However, the Fruity Chute was chosen as it was the only parachute readily available to the team with acceptable predicted performance to meet the kinetic energy requirement at landing.
- The black powder charges in the deployment system were reduced from 5g to 4, 4.5, and 5g after a ground test with 4g was completed. This was done to reduce the force exerted on the launch vehicle during ejection. The charge masses were also staggered as per the recommendation during the FRR presentation.

1.4.2 Changes to UAV Payload

The following changes were made to the UAV payload and deployment mechanism between the time of FRR and this test flight:

- The baud rate for the deployment transmitter was changed to 2,400 bps.

1.4.3 Changes to Air Braking System

The following changes were made to the ABS payload and between the time of FRR and this test flight:

- As a result of an issue with the shaft potentiometer, the decision was made to implement the ABS by fully extending the tabs when overshoot is detected rather than calculating appropriate partial extensions, since reliable position feedback was not assured. This will be discussed further later in the report.
- As a result of issues tuning the parameters of the Kalman filter to reliably and robustly filter the data of different data sets without considerable overshoot or undershoot, the decision was made to not use the Kalman filter in making decisions for the ABS in flight, as discussed further in the report.

2 Vehicle Demonstration Re-flight

2.1 Vehicle System Functionality

The vehicle system performed correctly, most notably shown with a steady flight as well as withstanding a large amount of force from the landing and sustaining minimal damage. The epoxy on the fin structure also cracked before the fin itself, which further prevented damage. Damage to the launch vehicle can be seen - and is addressed - in Section 2.4, below.

2.2 Recovery Subsystem Functionality

The deployment system functioned correctly, which causes the main and drogue parachutes to be ejected from the rocket at apogee. In addition, video from the transition section of the rocket provided visual confirmation that the Jolly Logic Chute releases remained connected until 500ft AGL at which point they released. Figures of the Jolly Logic Chute releases connected and unconnected during flight are shown in Figure 1.

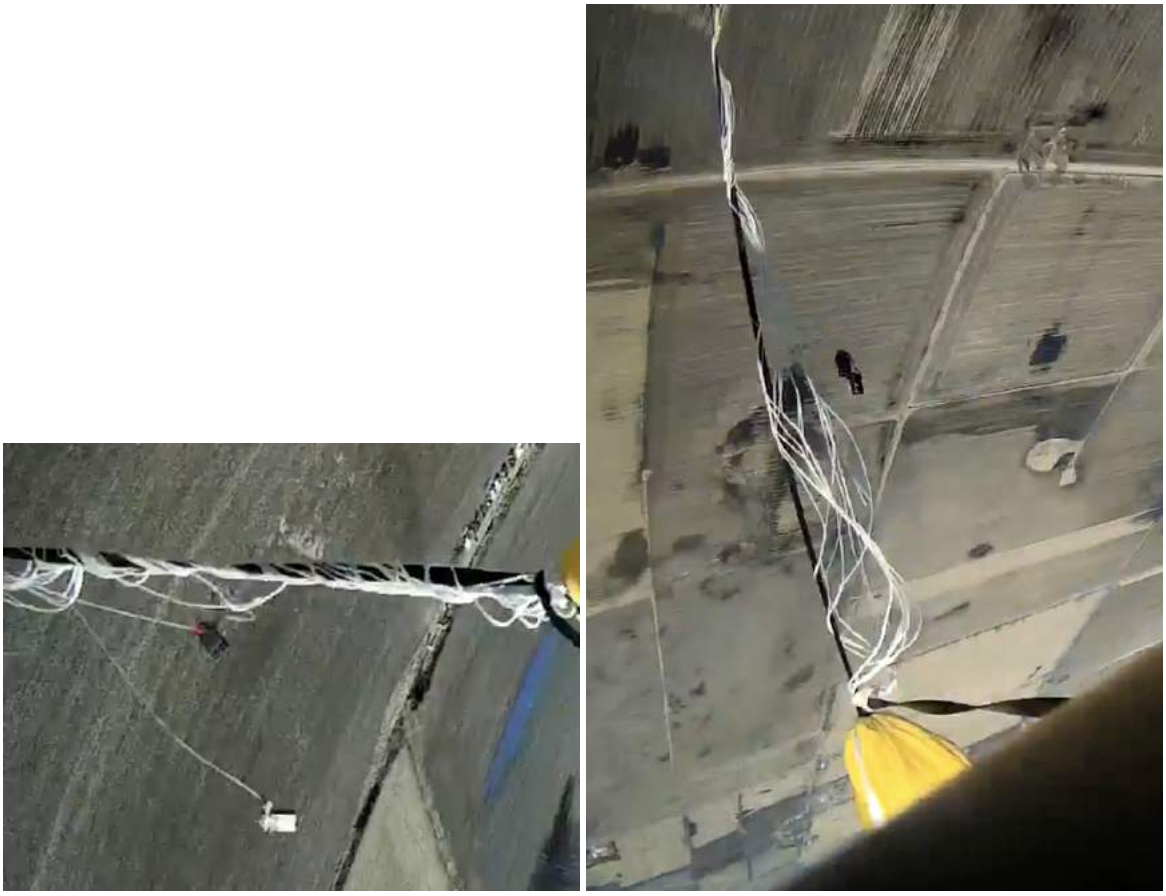

Figure 1: Chute Releases with different configurations during flight

However, shortly after apogee, the shroud lines of the parachute became tangled with the shock cord. The problem was further exacerbated by the spinning of the launch vehicle under drogue, which caused the shock cord to wrap around the main parachute. This prevented the main parachute from fully unfurling at 500ft AGL. Images of the tangled shock cord and shroud lines are shown in Figure 2.

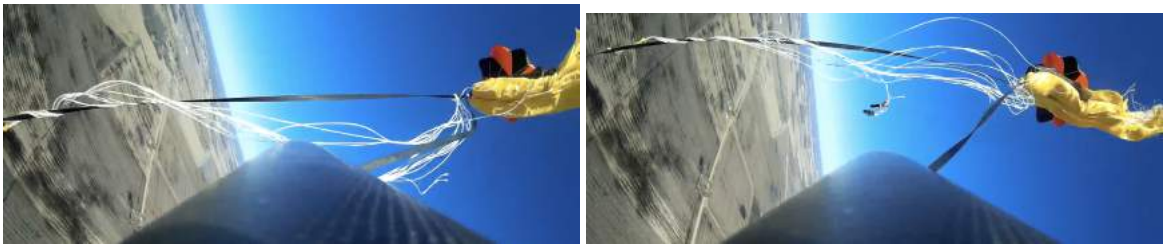

Figure 2: Tangled shroud lines preventing parachute deployment

This resulted in a final descent velocity of approximately 72.3ft/s, which provided a kinetic energy at landing of 2,079ft-lb. This landing was the cause of substantial damage to be discussed elsewhere in the report.

2.3 Analysis of Flight

2.3.1 Launch Day Simulation

The launch day conditions (see Section 1.3) were used to run OpenRocket and RockSim simulations for the as built launch vehicle. It was found that the predicted apogees from Open Rocket and RockSim were within 0.07% and 0.80% of the measured apogee during flight, as shown in Table 3. This further confirms that the simulation tools for the vehicle are accurate in predicting flight performance.

Table 3: Relevant altitude values

Method	Apogee [ft]	Max Velocity (ft/s)	Max Acceleration (ft/s^2)
Open Rocket	5,194	611	229
RockSim	5,231.76	610.27	230.44
Altimeter 1	5,200.6	672.6	2822.5
Altimeter 2	5,182.9	693.4	3962.6
Altimeter 3	5,188.2	693.8	2853. 6

From this model an overall drag coefficient of the rocket was found to be approximately 0.182. This was used to run a post flight simulation using an Euler method simulation written in a Matlab script for descent under drogue only. The result of this is shown in Figure 3. As shown, the Euler method simulation nearly perfectly models the experimental flight, which gives confidence in the ability of the team to model future flights using this tool.

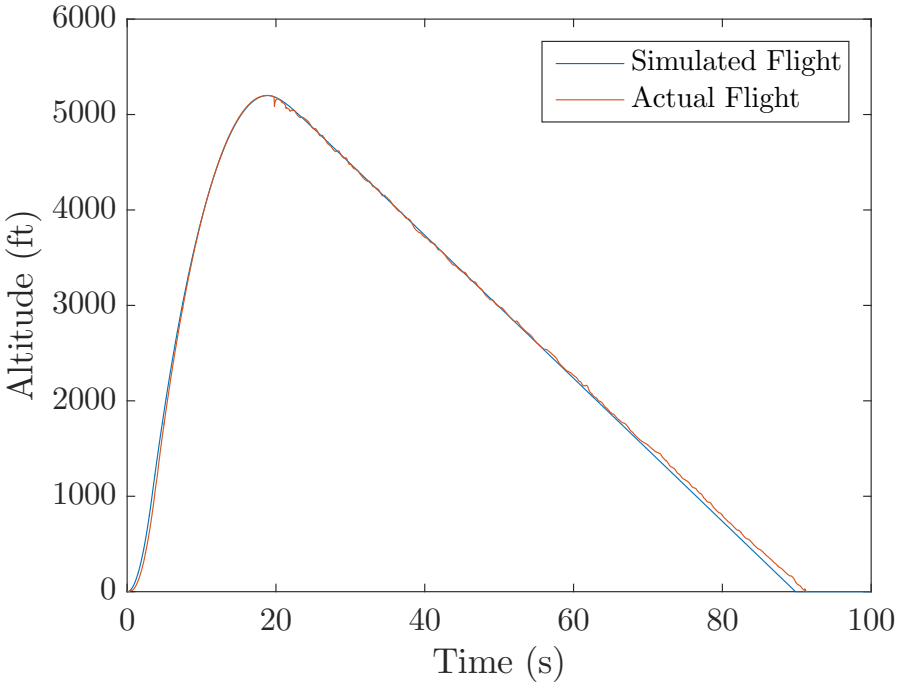

Figure 3: Simulated flight compared to measured flight

The predicted maximum velocities were 11.01% and 11.11% lower than measured, which is possibly due to noise in the signal. The maximum acceleration was an order of magnitude greater than predicted. This was due to the large acceleration at landing, which was not accounted for in pre-flight simulations. However, post flight simulations were able to account for this and provide an estimated kinetic energy at landing of within 2% of measured during flight.

2.4 Vehicle Damage and Path Forward

Aft Motor Centering Ring Warped

Upon vehicle impact, the off-nominal forces of landing bent one side of the aft centering ring in the body tube and cracked the epoxy adhering it to the fin can. This is problematic for two reasons, (1) the centering ring being skewed in the airframe induces tension on the motor mount that prevents the removal of the motor casing, and (2) the centering ring is no longer structurally sound. The team deemed it necessary to remove this centering ring through various methods of drilling and use of a Dremel to separate it from the airframe. A portion of the ring attached to the motor mount was left in order to provide a guide and additional structural support for a new aft centering ring to be integrated. This process can be seen in Figure 4, below.

Figure 4: Centering Ring post-removal

The new centering ring must fit directly onto the motor mount, however, the motor retainer has a larger outer diameter than the motor mount. Since the motor retainer adaptor cannot be removed, the inner diameter of the centering ring must increase to provide clearance. This creates a gap between the centering ring and motor mount tube. The team will resolve this by filling the gap with duct seal covered in JB Weld epoxy. The new centering ring will then be located above this base and braced against the portion of the old centering ring remaining in the airframe. This provides sufficient structural support for the fin can. It is worth noting that the motor mount itself did not move during the landing, nor were any other centering rings damaged. Therefore, it will be sufficient to use a new centering ring, and use the remains of the old ring as a crutch and a guide.

Fin Epoxy Cracked

On impact, the epoxy fillet adhering one of the fins to the outside of the fin can and to the motor mount cracked. The fin itself appeared intact on visual inspection, but the team decided to remove it to verify there was no further damage. The fin was removed by gently tapping with a rubber mallet to break any remaining epoxy connections such that it could be pulled free by hand. The fin was then sanded down first using a belt sander and then by hand to remove all surface epoxy. The epoxy remaining on the fin can and the motor mount will also be sanded off by hand. The same fin will then be re-adhered to the airframe in the same manner described in the FRR. It will use JB Weld where the fin touches the motor mount and RocketPoxy where the fin touches the fin. Since the aft centering ring was removed, the team will have access to this part of the rocket to properly fillet all contacting surfaces. The team will use the fin alignment rings described in the FRR to ensure the fin is adhered at the right angle. Figure 5, below, shows the removed fin as well as the open slot on the fin can.

(a) Fin, post-launch (sanded) (b) Empty slot of removed fin

Figure 5: Fin Can after fin removal

Motor Casing Removal

After landing, the motor casing became stuck in the airframe and could not be easily removed from the motor mount tube. This was due to the aforementioned structural failure of the aft centering ring. However, the vibration caused by drilling and use of a Dremel to remove the centering ring caused the stuck motor casing to be dislodged. Removal of the centering ring then resulted in the casing to be easily removed and cleaned by the team mentor for future flights.

Bent ABS tie rods

The four tie rods used to integrate the ABS were significantly warped due to the landing impact such that the ABS could not be pulled smoothly out of the fin can. The force required to dislodge the payload led to the system breaking into two pieces. The majority of the payload was dislodged and intact, however the spacing struts were sheared, leaving a single HDPE bulkhead that was removed separately.

In order to repair this damage, the tie rods will be hand-straightened as much as possible. However, because they cannot be straightened enough to work with the current system, the size of the clearance holes on ABS plates will be increased to allow more tolerance in the linearity of the rods. This allows the system to be easily inserted and removed again. Additionally, collars will be added to the top of the ABS that will tighten around the rods enough to fully secure and center the system within the fin can.

Nose Cone

The fore section of the separated rocket landed directly on the nose cone causing significant cracking damage of the nose cone. The nose cone was deemed irreparable due to the extent of the damage, so a new, identical nose cone has been ordered. The damage received by the nose cone is shown in Figure 6

Figure 6: Nose Cone Damage

2.5 Recovery Subsystem Path Forward

During the March 22 flight, the Fruity Chute Iris Parachute was used in order to explicitly meet the kinetic energy at landing requirements in the NASA Student Launch Handbook during this vehicle demonstration re-flight. It was off design from the Rocketman 20 foot Standard parachute, but was selected due to the vendor being unable to supply the Rocketman parachute in time for the launch. The team had previously conducted a launch using a Rocketman 14 foot parachute, but this was deemed unfeasible for the context of this flight due to the high descent rate not explicitly meeting the NASA requirements. The parachute to be used in competition is the Rocketman 20 foot chute, which is expected to arrive before March 26, so that it can be adequately tested before the flight in Huntsville. The dynamics and performance of the Rocketman parachutes are well know. The team has demonstrated that accurate estimation of descent velocity and drift radius can be calculated. For the March 2 launch, a post simulation flight was compared to the experimental data and is shown in Figure

7.

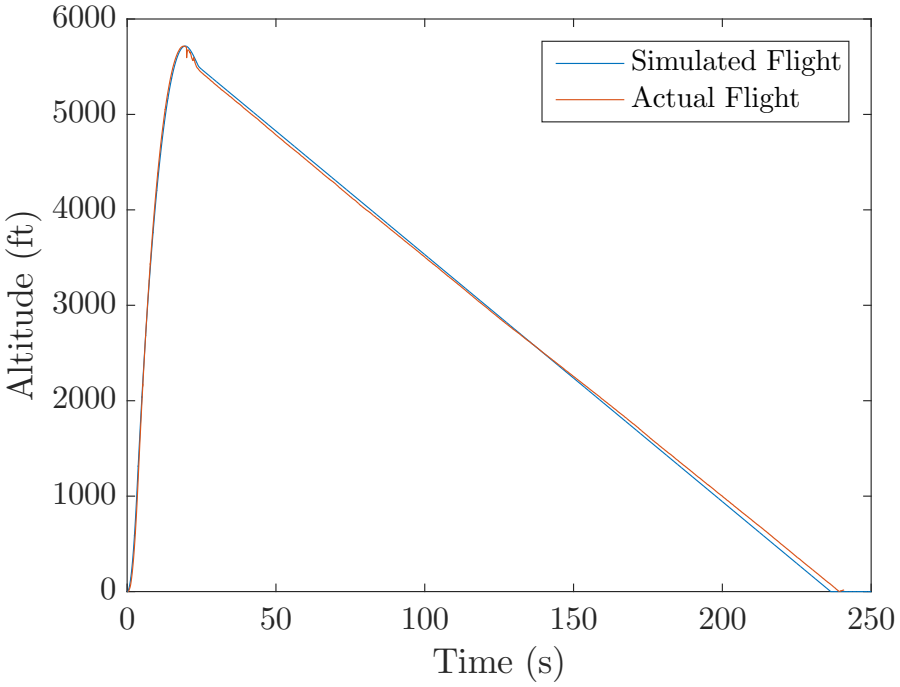

Figure 7: March 2 flight data compared to simulated data

As shown in the Figure, the modeling tools for the flight profile are extremely accurate. For this reason, the team is comfortable using the Rocketman 20 foot parachute during competition. This parachute consists of only 4 shroud lines compared to the Fruity Chutes' 36, drastically reducing the risk of the lines becoming tangle during flight. In addition, the most likely failure mode of the Rocketman chute results in a full deployment of main at apogee as compared to the most likely failure mode of the Fruity Chute, which results in no main deployment. The team fully believes that the Rocektman chute is not only the safer option, but also the more reliable.

In order to prevent the main parachute from interfering with the drogue chute during descent, the main parachute will also be connected to a extender shock cord 5 feet in length. The extension is intended to separate the main chute from the primary harness and allow for uninhibited use of the chute releases. A comparison of the previous setup in flight and the path moving forward is shown in Figure 8

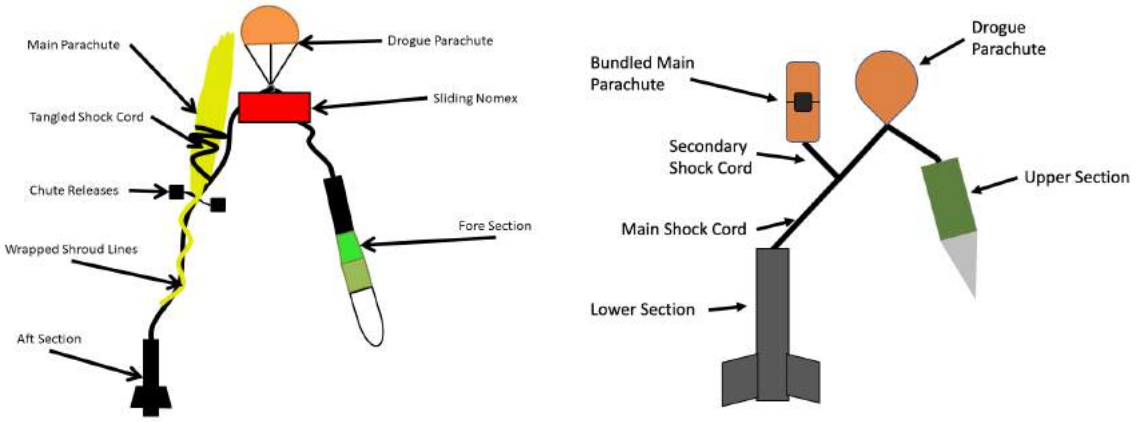

Figure 8: As launched schematic (left) vs. the new design (right)

In order to mitigate the failure mode which caused main deployment at apogee on the March 2 launch, the parachute will be packed such that the shroud lines are wrapped around the bundled parachute. This prevents the shroud lines from being pulled out of the parachute bundle when the shock cord is pulled. Finally, The Jolly Logic Chute Releases will be tied directly around the parachute, instead of around the Nomex protector. This will mitgate the risk of main deployment being induced from separation of the packed chute from the Nomex bundle and will ensure a more secure fit during ejection. A comparison of the two folding methods are shown in Figure 9.

Figure 9: As launched packing (left) vs. the new packing method (right) Photos courtesy of Rocketman Enterprizes and Fruity Chutes Inc.

2.6 Lessons Learned

Vehicle Design

The lesson learned from this demonstration flight is that when adhering two components together, it is ideal that the adhesive be strong, but not stronger than the components themselves. This is so that on impact, the adhesive connecting the components will fail prior to the component itself cracking or fracturing. This will not only lead to predictable failure modes but will also save time and money when repairs are necessary.

Recovery Design

The parachute packing is paramount to the success of the recovery subsystem, especially when the parachute is exposed to the air stream for a substantial time due to the chute release. Better packing ensures correct unfolding, and full deployment of the parachute during descent. Minimizing the number of shroud lines is also an important factor in reducing the tendency to tangle.

3 UAV Payload Demonstration Flight Results

3.1 Payload Retention

3.1.1 Design Summary

The Unmanned Aerial Vehicle Payload consists of the deployment system, the drone platform, and the drone itself, where the deployment system and platform are responsible for the proper retention of the UAV. The deployment system is screwed into the rocket from outside the body tube and functions in two stages: Orientation Correction and Linear Transport. Photos of the deployment electronic components may be found in Figure 10.

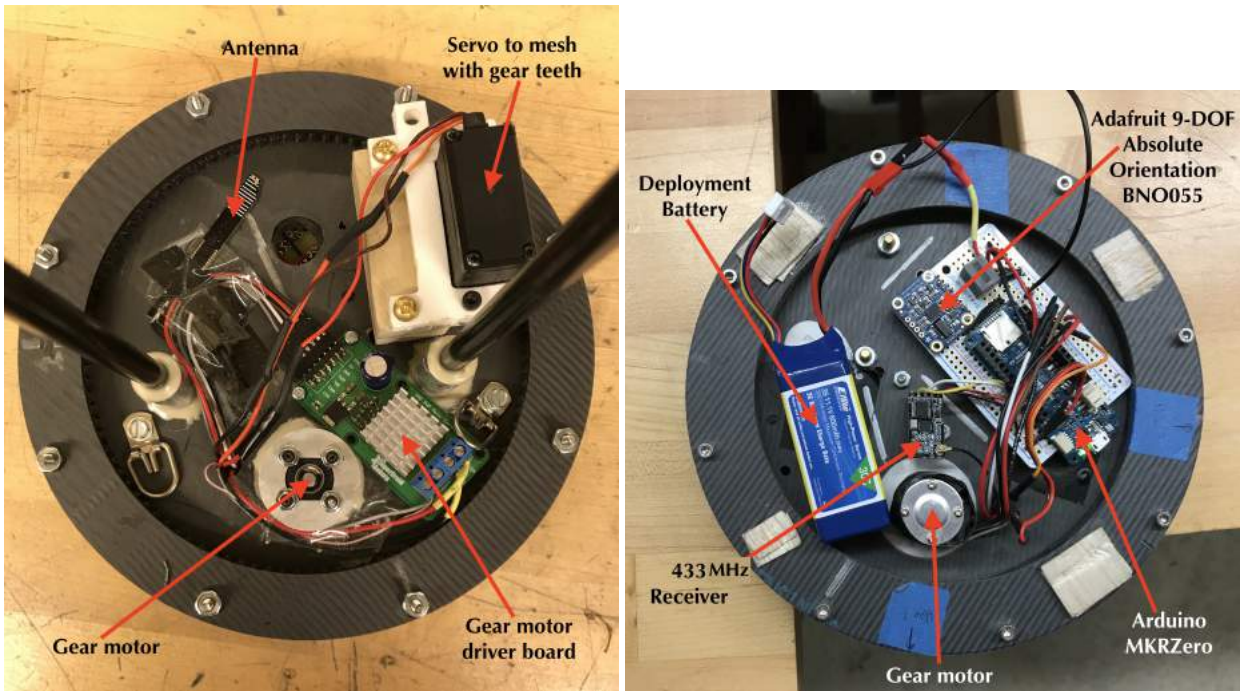

(a) Front of aft bulkhead assembly.

(b) Back of aft bulkhead assembly.

Figure 10: Deployment electronics.

After receiving a signal, the Orientation Correction sequence of the deployment process occurs first. Orientation Correction is driven by readings from the BNO055 sensor. The servo reorients the entire system (drone and platform included) according to this BNO055 reading. For the duration of the flight and prior to receiving a remote activation trigger, given under the supervision of a Remote Deployment Officer, the servo acts to lock the rotating bulkheads and, therefore the entire drone, in one orientation within the airframe. The retains the entirety of the UAV payload radially within the payload bay. In addition, a nylon leadscrew is attached to the shaft of the 116 RPM Actobotic Gear Motor. After reorientation, the Arduino MKRZero sends a signal to the gear motor to turn the leadscrew for Linear Transport. Throughout flight, however, the gear motor locks the leadscrew in place. By preventing rotation of the screw, the UAV and nose cone are secured along the axis of the airframe.

The leadscrew is the only component attaching the nose cone to the payload bay and is responsible for its retention. Because the nose cone remained attached to the payload bay throughout launch and recovery, this system is determined to be successful in retaining the payload. Additionally, the deployment mechanism is secured to the airframe via six screws running through the payload bay into the aft bulkhead of system. These screw show no evidence of yielding or significant wear after the flight. The payload components (deployment, UAV, nose cone, and platform) all therefore are shown to be properly retained. The payload bay post launch and recovery may be seen in Figure 11.

Figure 11: Nose cone still securely attached.

3.1.2 System Functionality

Due to unsuccessful main parachute deployment on Saturday, March 23, it is unclear as to whether or not the deployment sequence of the payload would have functioned as intended. The deployment sequence includes Orientation Correction and Linear Transport, where the Linear Transport sequence includes disengaging the UAV from its platform and powering on the UAV. Successful disengagement of the UAV from its platform occurs during linear translation when all four R-clips are pulled out of the aluminum flanges and, thus, each strut of the UAV. Photos of this process are found in Figure 12.

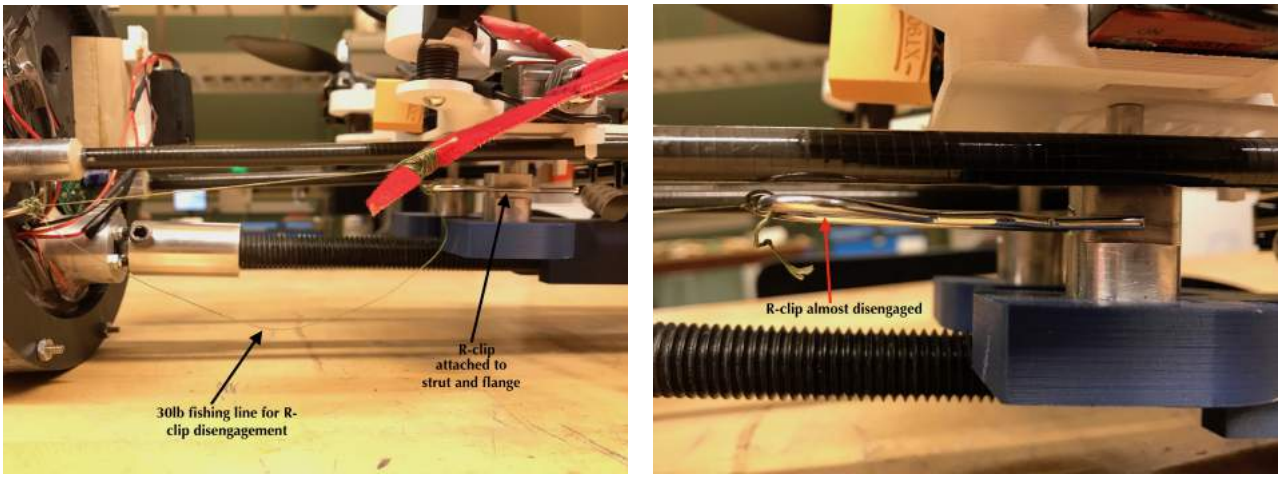

Figure 12: R-clip engagement before and after Linear Transport.

Because the UAV was not deployed during the launch on March 23rd, the R-clips were never pulled from the struts of the UAV. However, the R-clips were successful in keeping the UAV restrained for the entirety of launch and recovery. Successful activation of the UAV also occurs during linear translation. Similar to the disengagement of the UAV, fishing line attached to the aft bulkhead becomes taut as the UAV moves forward, thus pulling the switch on the UAV and powering on the drone. Photos of this process are found in Figure 13.

(a) Setup before powering on. (b) Powered off. (c) Powered on.

Figure 13: UAV power-on sequence before and after Linear Transport.

Because the UAV was not deployed yesterday, the UAV was never powered on. However, this mechanism was successful in preventing the premature activation of the UAV for the entirety of launch and recovery. It is therefore shown, that for the duration of the flight, all UAV components were successfully retained and the UAV remained in a powered off state.

3.1.3 Plan of Action

As a result of the impact at landing the following hardware experienced structural failures which are also shown in Figure 14:

- The nylon leadscrew was sheared just aft of the nose cone. A replacement for this component has already been ordered from McMaster Carr. This component will remain unchanged only replaced.
- Carbon Fiber rod aiding in orientation correction to rotate the sled broke. A replacement has been ordered from Rock West Composites and remaining material in the aluminum flange shall be drilled out in order to avoid milling a new nylon bulkhead.
- A single drone platform arm broke. There exists funds in the budget to 3D print a replacement within 3 business days from the Innovation Park at Notre Dame. The current component can also be repaired using JB Weld epoxy and a dowel rod insert for added structural integrity.
- Drone platform itself experienced a single arm breaking. A replacement shall also be 3D printed at Innovation Park.

Figure 14: Broken hardware for this year's scoring payload.

The R-clip driven retention mechanism was successful in keeping the entire drone attached to the platform throughout the entirety of flight. The broken arm most likely fractured due to the way the drone sits inside the payload bay. Its arms and props rest against the inner wall of the body tube, so impact at 87 G's exceeded its shear strength. A figure showing the interface between the props and the inner wall of the body tube is the following, Figure 15.

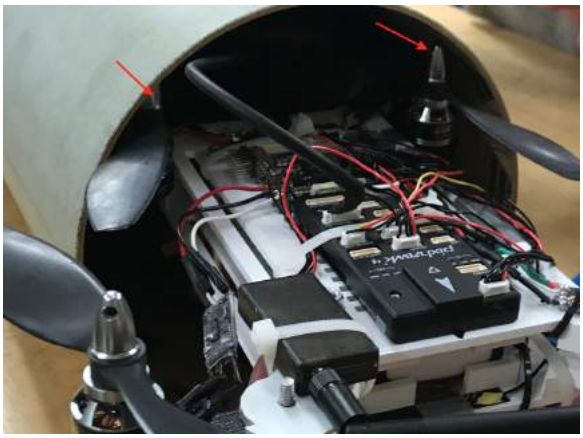

Figure 15: Red arrows highlight the points where the drone touches the inner wall of the body tube.

It is important to note that NASA Deployable Unmanned Aerial Vehicle (UAV) / Beacon Delivery Requirement 4.4.10. was respected during this second full-scale test launch: Teams will ensure the UAV's batteries are sufficiently protected from impact with the ground. Not only did the Turnigy 4500 mAh drone Li-Po battery survive but also the 800 mAh deployment system Li-Po battery. Therefore, the system is capable of fully retaining the UAV and batteries for nominal flight loads.

3.1.4 Lessons Learned

In the future, the motor caps shown in Figure 15 will be replaced with lock nuts. Since the lock nuts are shorter, they will not rest against the inner wall of the payload bay. This will help extricate the prop arms as much as possible from launch vehicle wall vibrations during flight. It is worth noting that, while the other broken components (leadscrew, the carbon fiber tube, and the platform) experienced failures, all were previously flown on the March 2 launch and were successful. Thus, these components will not be changed during rebuilding.

3.2 Payload Mission

3.2.1 Summary of Mission Sequence

The following items have been deemed qualifications for a successful payload mission at the 2019 NASA Student Launch Competition.

1. The payload shall be powered off until the rocket has safely landed and has been approved for remote-activation by the Remote Deployment Officer.
2. The payload shall remain retained inside the vehicle utilizing a fail-safe active retention system.
3. The payload shall deploy from inside the launch vehicle from a position on the ground.

4. The payload shall fly to a NASA specified Future Excursion Area.

5. The payload shall drop a simulated navigational beacon on the Future Excursion Area and then shall move a safe distance away from the Future Excursion Area.

The mission sequence of the UAV payload and the mission sequence of payload retention work closely together. Therefore, Figures and notes in the Payload Retention section will be referenced in this section.

3.2.2 System Functionality

The UAV itself was shown to remain powered off for the entirety of flight since the deployment sequence was not autonomously triggered, and the UAV was unable to translate linearly out of the rocket, Figure 13. This shows that the UAV shall remain in the powered off state until deployment has been approved by the RSO. In addition, the payload was retained inside the vehicle for the entirety of flight, Figure 12. Due to an unsuccessful recovery, the payload was unable to deploy from a position on the ground nor was it able to fly to a specified Future Excursion and deliver the simulated navigational beacon. The remote activation was sent to initiate the deployment sequence; however, the aforementioned structural failures resulting from landing prevented full execution. Concerning the beacon delivery; it is worth noting that during previous testing, it has been shown that the Raspberry Pi Camera Board v2 and the FEA detection software have been proven to detect the yellow FEA target. Additionally, the UAV has been able to achieved successful and stable manual flight.

3.2.3 Plan of Action

The flight conditions experienced during the recovery stage of this test flight prevented the payload from completing Mission Success Criteria 3, 4, and 5, as may be seen in Figure 14. The team will therefore implement the aforementioned repair methods listed in Section 3.1.3 and rebuild the drone in the configuration flown on March 23. Additionally, the team will continue implementing further ground tests of the Orientation Correction System and the Linear Transport System. Supplemental testing of the mission sequence and UAV deployment shall continue to be conducted post-launch to verify that all electrical components function as intended and suffered no damage as a result of impact. Notably, both Li-Po batteries were completely intact and in working order. If errors are found in these batteries during testing this week, replacements will be purchased immediately.

As far as flight and payload mission go, the drone will be reprinted with 100% infill at Innovation Park at Notre Dame to prevent the arm from fracturing again. The other subsystems in the payload shall be further tested for intended functionality. Additionally, FEA data will continue to be gathered via laptop as the drone itself is being rebuilt and mounted to continue to improve the. Once the drone is remade (by Thursday, March 28), the team will fly it and continue to test the Beacon Deployment Subsystem.

3.2.4 Lessons Learned

It would have been wise to fly the ballasted version of the drone in the first full scale test with not only the fully assembled deployment system but also with fully functioning electronics. It would have been a good test to deploy the ballasted drone from the body tube post-recovery in order to check the Orientation Correction System and the Linear Transport System operation post-flight. Moving forward, the team will place emphasis on designing more effective tests of software and system responses as well as allocate more time for ballasted test flights to prevent risks to the sensitive drone electronics.

4 ABS Payload Demonstration Flight Results

4.1 Payload Retention

4.1.1 Design Summary

The payload retention system for the Air Braking System (ABS) consists of 4 steel threaded rods epoxied to a bulkhead in the fin can. These rods are positions to align with holes cut in the ABS bulkheads that secure the system and provide alignment of the drag tabs with the slots cut in the fin can. The threaded rods are secured using #10-32 hex nuts to lock in the top bulkhead of the payload.

The Air Braking System was also used to provide space for ballast. Ballast was placed in on the upper surface of the aft bulkhead of the system, and to the top of the fore bulkhead. These ballasts were secured using duct tape to the ABS component. The fore of the ABS retention and the ballast in that section are shown in Figure 16.

Figure 16: ABS Integration and Ballast

4.1.2 System Functionality

The ABS payload and ballast components were successfully retained in the fin can. As a result of the the main parachute not fully deploying, the fin can hit the ground at higher speeds than expected. This resulted in slight warping of the rails and with the added diameter on the aft bulkhead due to duct tape retaining ballast, the system became jammed in the airframe. The ABS was successfully removed from the fin can, but the threaded rods were further warped in the process. The integration rods post-launch are shown in Figure 17. Overall, the retention system functioned as intended, however, will need slight repairs.

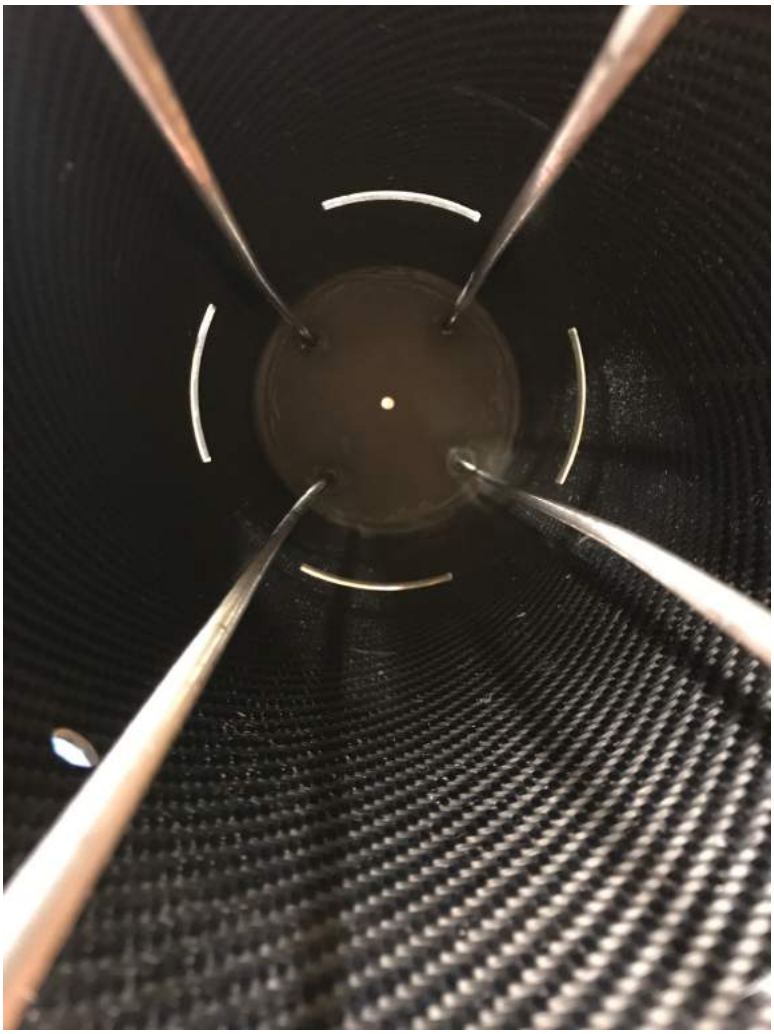

Figure 17: ABS Integration Rods Post-Launch

4.1.3 Plan of Action

The threaded integration rods that became warped during flight will be bent back as much as possible. Understanding that this may not mitigate the problem, the holes in the ABS bulkheads will be filed to a slightly larger diameter, allowing the threaded rods flexibility to move and prevent subsequent jams. This will be done incrementally such that they will not inhibit the retention and orientation of the system. If the rods cannot be properly aligned during the repair process, the bulkhead will have to be cut out and a new bulkhead and rods epoxied in. The aft bulkhead of the system will be sanded along the edges to allow additional space for the duct tape thus reducing the risk of another jam.

4.1.4 Lessons Learned

The results of this flight highlighted some of the possible downsides of this integration design. Because the threaded rods run directly through the ABS payload, jamming of the lower

bulkhead and damage to the threaded rods resulted in the entire system being temporarily stuck in the fin can. In future design iterations, the integration strategy will have to be reconsidered to avoid these risks and allow for easier access to the payload in the event of this type of failure. Potential alternatives include a twist to lock mechanism or screwing the payload into place via external screw ports in the fin can.

4.2 Payload Mission

4.2.1 Summary of Mission Sequence

The ABS is a vehicle payload which implements a control system to assist the vehicle in reaching the designated apogee. The system progresses through 5 stages: waiting, liftoff, motor burnout, apogee, and landing. The system is designed to remain idle until motor burnout occurs, and then compare recorded altimeter and accelerometer values to a predicted ideal flight reaching the target apogee of 4,700 feet for a given mass and motor selection. At apogee, the system is to retract the tabs fully and they shall remain retracted for the remaining duration of the flight. Recorded flight data and state machine decisions are recorded on a microSD card. The Air Braking System as built is shown in Figure 18.

Figure 18: ABS Assembly

4.2.2 System Functionality

4.2.2.1 Mechanism

The ABS mechanism successfully functioned during flight. As shown in figure 19, the tabs were fully extended for a portion of the flight occurring after motor burnout. This demonstrated the operation of the mechanism and that the launch vehicle remained stable during this extension. However, due to a software error discussed later in this report the tabs were prematurely retracted and did not remain extended throughout the ascent phase of flight. As a result, the ABS had a limited impact on the recorded apogee when compared with the simulated results using OpenRocket and Rocksim. The mechanism has been ground tested following the flight and was shown to still be operational.

(a) Tabs Retracted (b) Tabs Extended

Figure 19: ABS tab actuation during flight

4.2.2.2 Electronics

The ABS Electronics performed as expected. During pre-launch procedures, the power and status LEDs were properly illuminated, and the flight demonstrated the ability of the electronics to distribute power from the 7.4 V battery to the servo motor and Arduino-sensor system through a 5V voltage regulator. The servo motor and mechanism performed as designed and the system did not lose power during flight as indicated by the continuous data recorded on the SD card. The power and status LEDs were also observed through the vent holes to still be illuminated at the time of recovery, further indicating the system remained powered, as shown in figure 20. In order to mitigate issues with zip ties shearing during the first flight, the battery was retained in a custom 3D printed case epoxied to the electronics deck of the ABS. In addition to the case cover, the battery was secured by a velcro command strip and was successfully retained during flight. The new case is shown in Figure 21.

Figure 20: ABS Status LEDs at Recovery

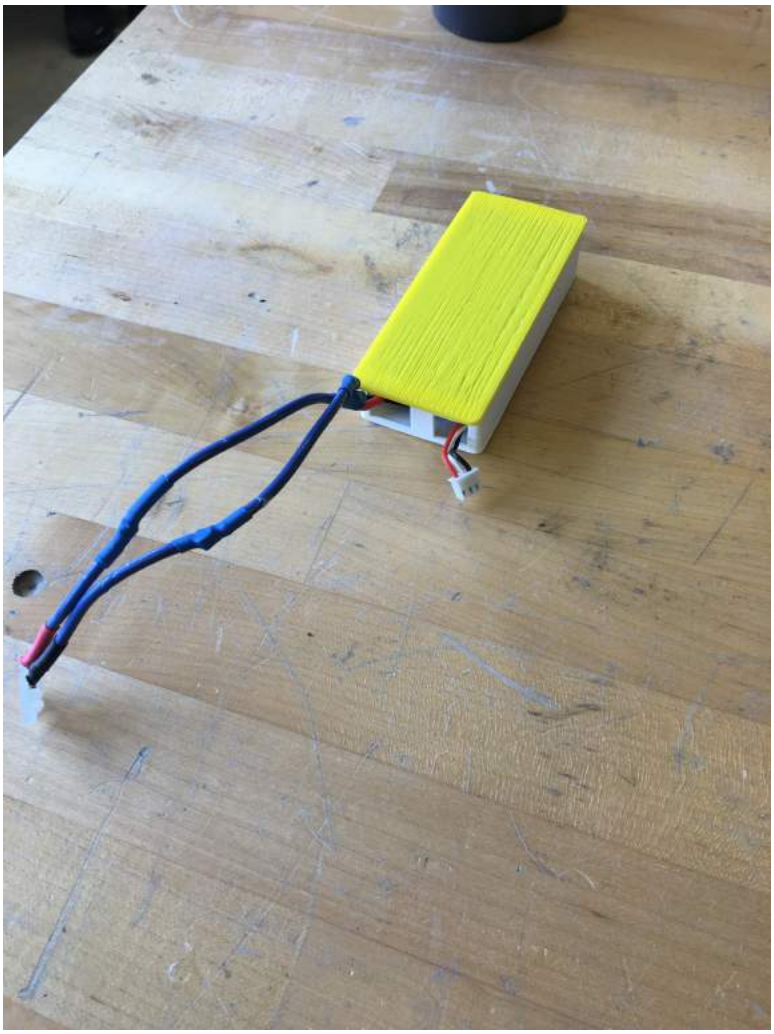

Figure 21: ABS Battery Case

There were two issues identified with the electronics prior to launch which impacted the system design. Firstly, the Arduino board used was receiving inconsistent initial values from the shaft potentiometer used to detect rotation of the mechanism. During testing, the potentiometer would record a different retracted value between tests. A possible fix was considered to record the initial retracted value as a reference, but the range of values from retracted to extended varied slightly depending on which value the system started at. As a result, the potentiometer was deemed unreliable for providing precise measurements of the shaft rotation. To counter this, the system was changed to fully extend the tabs when deemed necessary, and fully retract when not, rather than using the PID control for partial tab extensions which would have relied on the potentiometer values. The potentiometer values do change due to rotation, so this change is still utilized in detecting a jam.

The second issue identified after the first test flight is an issue with the accelerometer readings. The accelerometer on the BNO055 IMU is rated for up to 16 G's of acceleration. However, during motor burn the acceleration readings appear to hit a cap at 3 G's indicating the sensor does not perform to the highest rating expected. However, at values below 3 G's the

accelerometer appears to perform as expected, recording an average of 1 G downward after motor burnout. Additionally, the sign of the acceleration is measured properly which allows for successful state transition from liftoff to burnout which was demonstrated in this flight. As a result, the accelerometer still allows for normal system performance, but its rating issue should be noted.

4.2.2.3 Software

4.2.2.3.1 Kalman Filter Decision

Prior to launch the decision was made to remove the use of the Kalman filter. In testing the team could not find a reliable trust matrix that closely matched the path of previous launches when applied to multiple data sets. When passed different simulation and former flight data sets, the filter would match the ascent path closely but result in an 50-100 foot overshoot in apogee which was deemed unacceptable. The team did not believe that the filter would create a reliable representation of the rocket's state when implemented at launch, inducing a risk of false detection of flight events. The Kalman filter was also reliant on both accelerometer and altimeter data, and it was recently discovered that the accelerometer would cap at roughly 30 m/s^2. Since the accelerometer input to the Kalman was not reliable to cover the full range of values expected in flight the team did not believe that the Kalman filter could produce reliable state estimations.

4.2.2.3.2 Flight Performance

The recorded altitude and acceleration data are shown in Figures 22 and 23. The measured apogee by the ABS altimeter was 5,225 feet, which was 25 feet above the apogee recorded by the scoring recovery altimeter of 5,200 feet, representing a 0.48% difference.

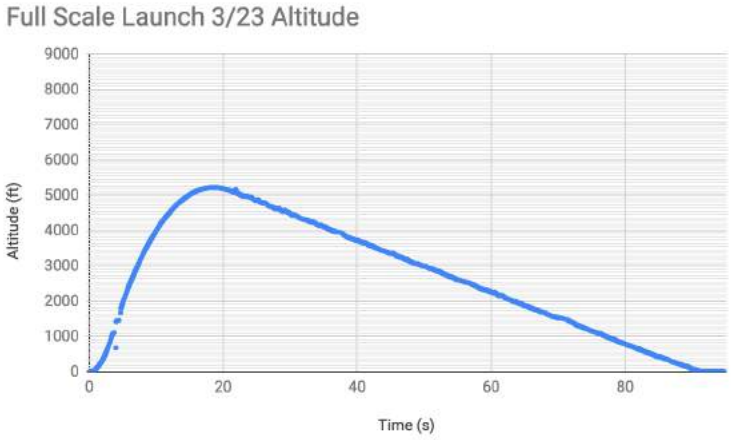

Figure 22: ABS Recorded Altitude

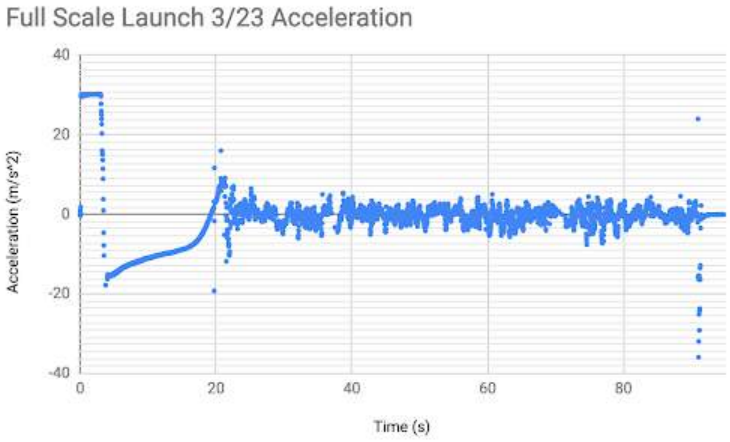

Figure 23: ABS Recorded Vertical Acceleration

The software was successful in processing and storing the recorded data and state transitions to the on-board SD card. The software was also successful in not deploying the tabs until after motor burnout had occurred as indicated by the video recording. Additionally, the system successful detected that the tabs needed to be deployed, as indicated by the vehicle ultimately overshooting the target apogee. It is worth noting that the sampling rate of the sensors was increased from 3 Hz in the previous flight to over 30 Hz in this flight. This was done by changing from the "SD.h" library to the "SDfat.h" Arduino library, and optimizing the points at which data is flushed to the SD card. However, when the motor is being rotated by a loop of code, the sampling rate decreases as seen in the apparent gap in data at approximately the 4 second mark in the altitude graph in figure 22. This is a result of an inefficiency of the code to sample sensors and actuate the system being run on the same controller at the same time.

The software experienced one issue that resulted in a premature detection of apogee and retraction of the tabs. Following motor burnout, the software successfully detected the tabs needed to be deployed and extended them into the airflow. Following this, the altimeter recorded a single noisy data point with a drop of 400 feet from the previous value, tripping apogee detection. An oversight was made when making the decision to remove the Kalman Filter, which was meant to counter these types of noisy data points and was not replaced by a separate simpler filter. This resulted in the system continuing to rely on just one decrease in altitude reading to trigger detection of the apogee flight stage.

4.2.3 Plan of Action

4.2.3.1 Software Mitigations

In order to mitigate the software detecting a premature apogee, two conditions will be added. The first is to check for numerous continuous samples of decreasing altitude and second is to incorporate the accelerometer in the decision. The latter is done by recognizing if the launch vehicle's axial acceleration has changed from the approximately negative 1 G at

burnout to a lower value as the fore of the vehicle begins to tip over at apogee.

Further, the criteria for every state transition will need to be met in five consecutive samples of the state machine in order to trigger a successful state transition. This will prevent sensor noise from triggering premature state transitions while also allowing state transitions to occur quickly. Second, calculations of velocity from sensor data will be averaged with the two previously calculated velocities so that decisions made regarding tab extension will be less susceptible to sensor noise.

To increase the sampling rate while the motor is actuating, the step size for the motor extension loop will be increased resulting in a faster extension and sampling rate. The speed of drag tab deployment demonstrated in this flight was deemed appropriate during testing, but faster deployment speeds have been tested and deemed reliable as well.

4.2.3.2 Pressure Sealing of ABS

Because the noisy data point indicating a drop in altitude occurred following the deployment of the tabs, it cannot be ruled out that the deployment of the tabs may have resulted in an unexpected pressure fluctuation within the airframe. In order to mitigate this potential issue, after inserting the ABS into the fin can duct seal will be applied to the drag tab slots to seal the gap between the drag tab section of ABS and the fin can. This would ensure that the only space exposed to the airflow are the three pressure taps located radially around the ABS altimeter.

4.2.3.3 Hardware Repairs

As a result of the issues described in the ABS Payload Retention section, the bottom bulkhead of the ABS was jammed in the fin can as a result of landing. In removing the ABS, two screws were sheared in the nylon standoffs connecting the bearing plate to the lower bulkhead. Therefore, these nylon standoffs will be replaced. The rest of the system hardware has been recovered and mechanically ground tested to perform nominally after the launch. The ABS as removed from the fin can with the bottom bulkhead detached is shown in Figure 24.

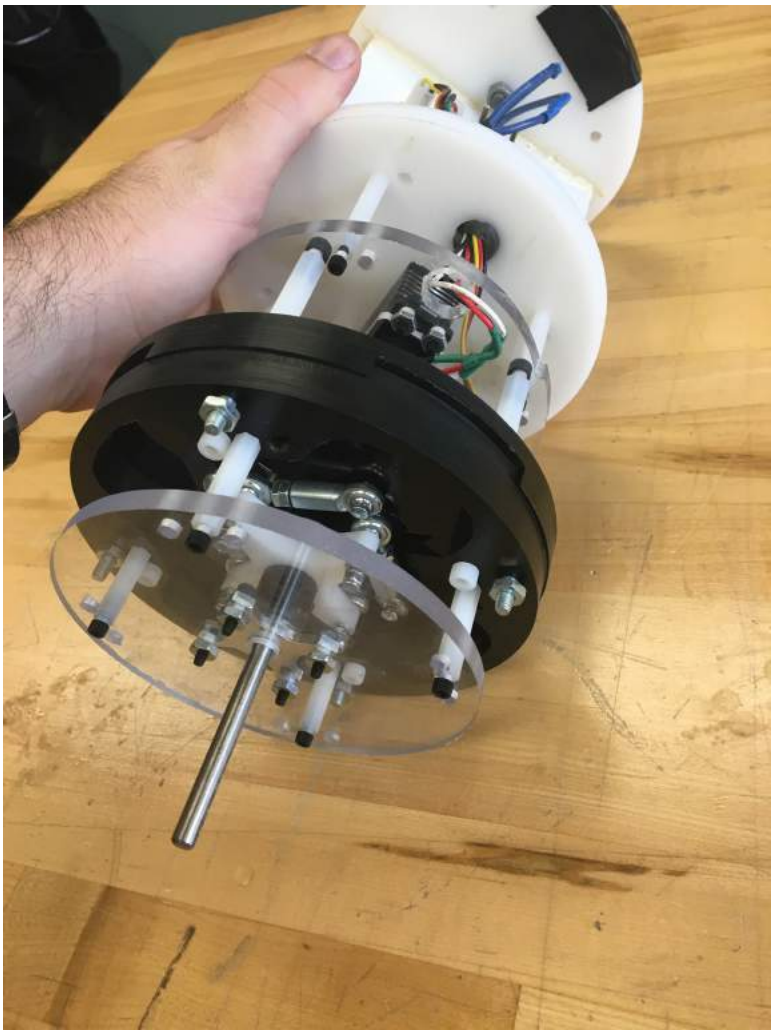

Figure 24: ABS Recovered

4.2.4 Lessons Learned

The flight demonstrated the importance of preparing robust tests for the conditions to make decisions and transitions system states. While simulated flights were performed on the ground to ensure the tabs would deploy as expected, more could be done to test the system with simulated data that has a noisy signal added to it. This flight has provided valuable data for understanding the performance of the payload components and will allow for adjustment of the software for more robust state detection conditions. Moving forward, the team will place special emphasis on learning how to design more effective tests of software and system responses.